#121A dupl

E/2/A

FERMILAB-PUB-74-141-E
UCD-PPL-6-15-74

SINGLE PION PRODUCTION IN π^+p AND pp COLLISIONS AT 100 GeV/c, A DETAILED TEST OF FACTORIZATION*

J. Erwin, Winston Ko, R.L. Lander, D.E. Pellett, and P.M. Yager

Department of Physics, University of California, Davis, California 95616

and

M. Alston-Garnjost

Lawrence Berkeley Laboratory, University of California, Berkeley, California 94720

Abstract

A relatively bias free comparison is made of the charged pion single particle spectra in π^+p and pp interactions at 100 GeV/c. Inclusive and semi-inclusive spectra are compared. Mueller factorization is seen to describe inclusive π^- production but not π^+ production. Factorization also applies to proton target fragmentation into π^- for a fixed number of backward π^- in the CM, but not for a fixed total number of π^-. $ab\bar{c}$ exoticity is found to be the exoticity form controlling the approach to factorization. In the central region, the $s^{-1/4}$ approach to factorization in $\pi^+p \to \pi^\pm$ is consistent with the approach to the same asymptotic value (~0.78) in other inclusive reactions.

*Work supported in part by the U.S. Atomic Energy Commission (AEC AT(04-3)-34 PA 191)

SINGLE PION PRODUCTION IN π^+p AND pp COLLISIONS AT 100 GeV/c, A DETAILED TEST OF FACTORIZATION

J. Erwin, Winston Ko, R.L. Lander, D.E. Pellett, and P.M. Yager

Department of Physics, University of California, Davis, California 95616

and

M. Alston-Garnjost

Lawrence Berkeley Laboratory, University of California, Berkeley, California 94720

In a Fermi National Accelerator Laboratory 30" bubble chamber experiment with an unseparated but tagged π^+ and proton beam at 100 GeV/c, we have a unique opportunity to compare the produced pion spectrum from π^+p and pp collisions with minimum biases.

When a pion is produced in the target fragmentation region, i.e. the center of mass rapidity of the pion is near that of the target (-Y/2), the inclusive cross section can be represented by the Mueller diagram in Fig. 1(a); in the diagram "b" represents the beam. If the pomeron dominates the link between the beam and the πp "blob", and if it is <u>factorizable</u>, the cross section can be written[1,2] in the form of a product,

$$\frac{d^2\sigma}{dydp_T^2} = \beta_{\pi p}\ (y,\ p_T^2)\ \beta_b. \tag{1}$$

This is analogous to the factorization in the total cross section, in Fig. 1(b),

$$\sigma_T = \beta_p \beta_b\ . \tag{2}$$

Now when we divide equation (1) by (2), the quantity

$$\frac{1}{\sigma_T}\ \frac{d^2\ \sigma}{dydp_T^2} = \beta_{\pi p}\ (y,\ p_T^2)\ /\ \beta_p \tag{3}$$

becomes independent of the beam. At finite energies, when there are Reggeon contributions to the diagram of Fig. 1(a), we have to add another term in equation (1)

$$\frac{d^2\sigma}{dydp_T^2} = \beta_{\pi p}\ (y,\ p_T^2)\ \beta_b + \beta'_{\pi p}\ (y,\ p_T^2)\ \beta'_b\ s^{-1/2}. \tag{4}$$

Then the quantity $\frac{1}{\sigma_T} \frac{d^2\sigma}{dydp_T^2}$ has an $s^{-1/2}$ dependence on the beam.

In the central region, where y is small, we can write the inclusive distribution according to Fig. 1(c)

$$\frac{d^2\sigma}{dydp_T^2} = \beta_p \beta_b \gamma(p_T^2) . \tag{5}$$

The height at the center of the distribution $\frac{1}{\sigma_T} \frac{d^2\sigma}{dydp_T^2} = \gamma(p_T^2)$ is independent of both the target and the beam. There is a $s^{-1/4}$ approach to this limit from the additional term[2)] to equation (5),

$$\frac{d^2\sigma}{dydp_T^2} = \beta_p\beta_b \gamma(p_T^2) + \beta_p' \beta_b' \gamma' (p_T^2) s^{-1/2} s^{-1/2} . \tag{6}$$

In the experiment we are reporting we use two different kinds of beam particles π^+ and p, and measure $\rho = \frac{1}{\sigma_T}\frac{d\sigma}{dy}$ in an otherwise identical experimental situation. The 30" was exposed to an unseparated beam of π^+ and p at a ratio of about 7:8. The identity of each individual incident particle is determined by a 35 m long differential Cherenkov counter and its location is tagged by three sets of Multiwire Proportional Chambers[11)]. As far as the scanning and measuring are concerned, however, π^+p and pp events are treated <u>identically</u>. The systematic difference is therefore minimized. The absolute cross section normalization is also not a problem, since we use

$$\rho = \frac{1}{\sigma_T} \frac{d\sigma}{dy} = \frac{1}{N_T} \frac{dN}{dy} . \tag{7}$$

where N_T is the number of total events in the data sample (corrected for 2 prong inefficiency). This experiment is therefore unique in its rather systematics-free test for factorization.

All the events are measured on the LBL spiral reader with an automatic track-match. Using a priori forward-backward symmetry in the c.m. for pp interactions, we can determine the efficiency for track matching and reconstruction in each of the hemispheres and for each topology. The tracks in the backward hemisphere in the center of mass have a good reconstruction efficiency, quite independent of multiplicity, of better than 96%. The efficiency for tracks going forward in the center of mass drops as the multiplicity increases, with 80% successfully reconstructed on the average. These efficiencies can be also applied to the π^+p samples. The number of tracks from π^+p events, computed after weighting with the efficiencies obtained from the pp interactions, is consistent with the number obtained in the scan count. This agreement holds for each topology separately. Thus track matching and reconstruction losses appear to be equal for pp and π^+p events.

To compare the spectra for produced particles from π^+p and pp interactions, it is most appropriate to take the ratio of the single particle spectra, for then the efficiency factor will divide out. We find (see Fig. 2) that for π^- the ratio

$$\rho_-(\pi^+p)/\rho_-(pp) = \frac{1}{\sigma_T}\frac{d\sigma}{dy}\ (\pi^+p \to \pi^-)\ /\ \frac{1}{\sigma_T}\frac{d\sigma}{dy}\ (pp \to \pi^-) \qquad (8)$$

is flat and almost 1 in the backward hemisphere in the c.m. system up to $y = -0.6$.[3] The ratio for all events with $y < -0.6$ is $0.98 \pm .04$. Factorization in the fragmentation region of the proton thus works remarkably well for π^-.

It is also interesting to see the ratio in the forward hemisphere rise approximately linearly. This ratio measures the difference in the structure functions of the two projectiles.

The fact that the ratio is a constant and consistant with unity in the backward hemisphere, shows that, at 100 GeV/c, the Pomeron dominates the process of Figure 1(a) and Pomeron factorization works to a remarkable 2% level. That is, the function $\beta_{\pi p}(y,p_T^2)$ in equation (3) has the same y dependence in π^+p and pp interactions. Furthermore, when we compare in Fig. 3(a) the average p_T as a function of y for these same two reactions, we see they are nearly the same at any value of y in the backward hemisphere. In Fig. 3(b) we make a comparison of the p_T distributions for events in the backward hemisphere. The ratio is again consistant with 1 for all p_T. Our conclusion is therefore that, in the inclusive reactions $\pi^+p \to \pi^-$ and $pp \to \pi^-$, factorization works; $\beta_{\pi p}(y,p_T^2)$ is independent of the projectile.

As we examine further the details of factorization, Fig. 4 shows that the ratio of equation (8) at a fixed multiplicity is <u>not</u> 1, or even a constant, at all multiplicities. The Mueller picture doesn't make any prediction about these ratios. However, if target fragmentation is indeed independent of the projectile, then the n_- multiplicity distributions in the target fragmentation region should be the same for π^+ and p projectiles.

It is therefore proper to examine the ratio in equation (8) at a fixed π^- multiplicity <u>in the backward hemisphere</u>. This is shown in Fig. 5. The ratios are constant and equal to 1 in the backward hemisphere.

It is indeed quite remarkable that factorization works in such a detail. There were indications of factorization at lower energies for the π^- fragments of the proton.[4] The agreements were usually good to 10%. Mueller's picture with a factorizable pomeron will give exact factorization. Some recent work on

a Geometric Model[5] can also give approximate factorization to 10%. The degree of factorization we have observed makes the Mueller picture look very good.

As a passing note of interest, we look at the π^- distribution (non-invariant) in the backward hemisphere, as a function of the Feynmann scaling variable $X = \frac{2P_L}{\sqrt{s}}$. As shown in Fig. 6, an exponential is a good description of the data, with slopes of 11.9 ± 0.5 and 11.7 ± 0.4 for π^+p and pp interactions, respectively. We notice these slopes are within 10% of the value at lower energies.[6] Feynmann scaling is good to 10% from 10 GeV/c to 100 GeV/c.

Returning to the rapidity distributions, we see that at $y_{cm} = 0$, the ratio of (8) is 10% above 1. As indicated in equation (6), there is an $s^{-1/4}$ approach to factorization in the central region, i.e. the pion production at $y_{cm} = 0$ is independent of both the target and the projectile. Indeed, if we follow Brown[7] and Alston-Garnjost[8] and a later compilation by Ferbel,[9] and plot the value of ρ at $y_{cm} = 0$ for charged pion production in π^+p and pp reactions against $P_{inc}^{-1/4}$ in Fig. 7(a,b), the extrapolation to $s = \infty$ is consistent with the hypothesis that all curves approach a single point. In other words, from equation (5), at $s = \infty$ and $y_{cm} = 0$,

$$\rho = \int \gamma(p_T^2)\, dp_T^2 , \qquad (9)$$

a constant independent of projectile.

The value of ρ at $y_{cm} = 0$ for produced π^+ is shown in 7(b). The inconclusive trend of the lower energy data is modified by the 100 GeV data to be consistent with the same extrapolation point as the produced π^-, although there still is room for quite a bit of variation.

The π^+ produced in the π^+p interaction are more numerous than those in the pp interaction relative to the total cross sections. Now if we look at the ratio

$$\rho_+(\pi^+p)/\rho_+(pp) = \frac{1}{\sigma_T}\frac{d\sigma}{dy}(\pi^+p \to \pi^+) \Big/ \frac{1}{\sigma_T}\frac{d\sigma}{dy}(pp \to \pi^+) \qquad 10)$$

we see in Fig. 8(a) that even in the target fragmentation region this excess persists. However, the ratio is still quite constant in y. Furthermore as shown in Fig. 8(b), the ratio between the average p_T of the π^+, like that of the π^-, is the same for all y in the π^+p and pp interactions. For π^+ production, factorization is not achieved yet at 100 GeV/c, but the two structure functions $\beta_{\pi p}(y,p_T^2)$ and $\beta'_{\pi p}(y,p_T^2)$ in equation (4) seem to have the same y and p_T^2 dependence.

A final remark concerning the exotic[10] natures of the reactions. Using the notation b + a → c + x, we may ask which of the combinations $ab\bar{c}$, $a\bar{c}$, $b\bar{c}$, and ab are exotic for each reaction. The results are summarized in Table I. We note that the two reactions $\pi^+p \to \pi^-x$ and $pp \to \pi^-x$ are simultaneously exotic only in $ab\bar{c}$, and these are the reactions for which factorization is satisfied. The other two reactions are nowhere simultaneously exotic, and factorization fails by ∿ 13% for these reactions. This result suggests that if exoticity plays any part at all, it is $ab\bar{c}$ exoticity that operates.

The cooperation of the Fermi National Accelerator Laboratory and in particular the personnel of the Neutrino Laboratory is acknowledged with pleasure. The Proportional Hybrid Consortium deserve thanks for their help in operating the tagger.

REFERENCES

1. A. H. Mueller, Phys. Rev. D2, 2963 (1970)

2. H.D.I. Abarbanel, Phys. Lett. 34B, 69 (1971).

3. The limit -0.6 is chosen in order that the data lie within 2 units of rapidity of the target.

4. For a summary of previous experimental work, see R. Lander, Proceedings at the Rochester meeting of the APS/DPF, 1971, pg. 71.

5. H. Cheng, J.K. Walker, T.T. Wu, Phys. Rev. D9, 749 (1974).

6. Winston Ko and R.L. Lander, Phys. Rev. Letts. 26, 1064 (1971).

7. L. Brown, Phys. Rev. D4, 2760 (1971).

8. M. Alston-Garnjost, Proceedings of the Davis Conference (1972) pg. 182, and M. Alston-Garnjost et al., Phys. Letters 39B, 402 (1972).

9. T. Ferbel, Phys. Rev. Letts. 29, 448 (1972).

10. H.M. Chan, C.S. Hsue, C. Quigg and J.M. Wang, PRL 26, 672 (1971); J. Ellis, J. Finkelstein, P.H. Frampton and M. Jacob, CERN preprint TH 1216 (1971).

11. J. Erwin et al., Phys. Rev. Letters 32, 254 (1974).

TABLE I. EXOTIC NATURE OF REACTIONS

$b + a \rightarrow c + x$	$ab\bar{c}$	$a\bar{c}$	$b\bar{c}$	ab	$\rho(\pi^+p)/\rho(pp)$
$\pi^+p \rightarrow \pi^-x$	yes	no	yes	no	$0.98 \pm .04$
$pp \rightarrow \pi^-x$	yes	no	no	yes	
$\pi^+p \rightarrow \pi^+x$	no	no	no	no	$1.13 \pm .03$
$pp \rightarrow \pi^+x$	yes	no	no	yes	

FIGURE CAPTIONS

Fig. 1. Mueller diagrams for (a) single pion production in the target proton fragmentation region (b) total cross section (c) single pion production in the central region.

Fig. 2. Ratio of $\rho_- = \frac{1}{\sigma_T} \frac{d\sigma}{dy}$ for inclusive π^- production in π^+p and pp interactions.

Fig. 3. (a) Ratio of the average transverse momentum of the π^- in π^+p and pp interactions.

(b) Ratio of transverse momentum distribution of the π^- in π^+p and pp interactions for all π^-'s backward in the center of mass.

Fig. 4. Ratio of ρ_- in π^+p and pp interactions at a fixed charge multiplicity.

Fig. 5. Ratio of ρ_- in π^+p and pp interactions for fixed number of π^-'s in the backward hemisphere.

Fig. 6. Distribution of π^- in $X = \frac{2P_L}{\sqrt{s}}$, in the backward hemisphere.

Fig. 7. (a) Value of ρ at $y_{c.m.} = 0$ for pion production in pp interactions with different incident momentum, as a function of $p^{-1/4}$.

(b) Same as (a) for π^+p interactions.

Fig. 8. (a) Ratio of ρ_+ for inclusive π^+ production in π^+p and pp interactions.

(b) Ratio of the average transverse momentum of π^+ in π^+p and pp interactions.

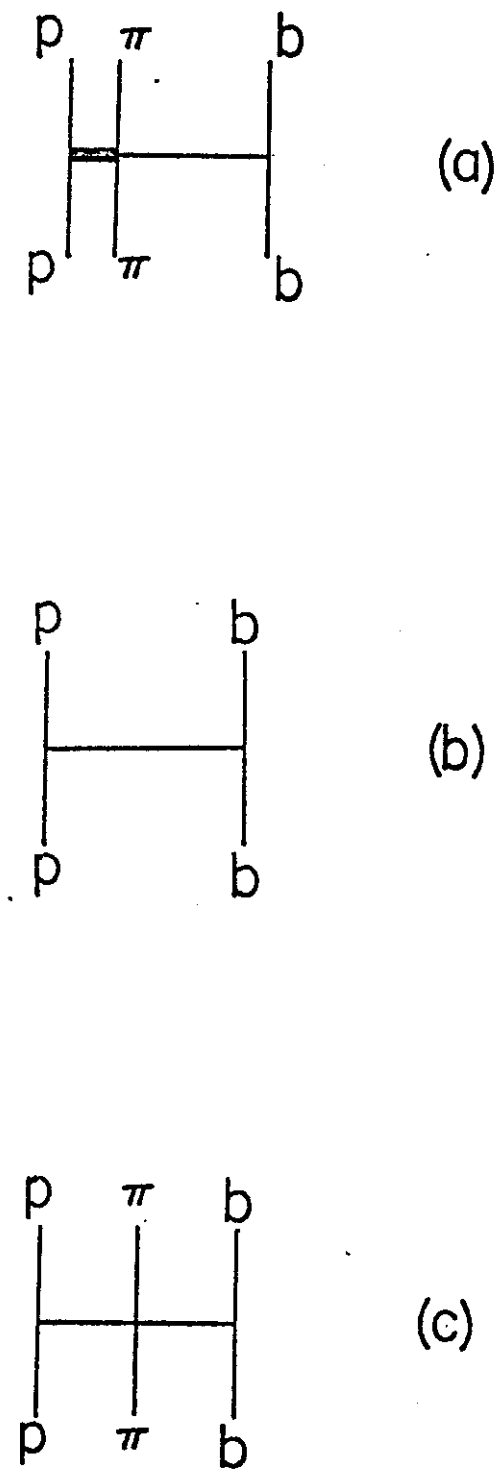

Fig. 1

100 GEV/C INCLUSIVE

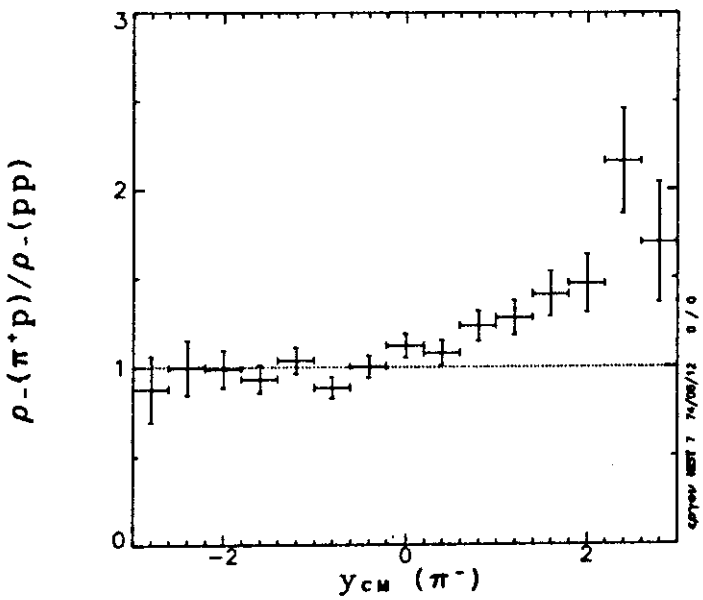

Fig. 2

100 GEV/C

π^-

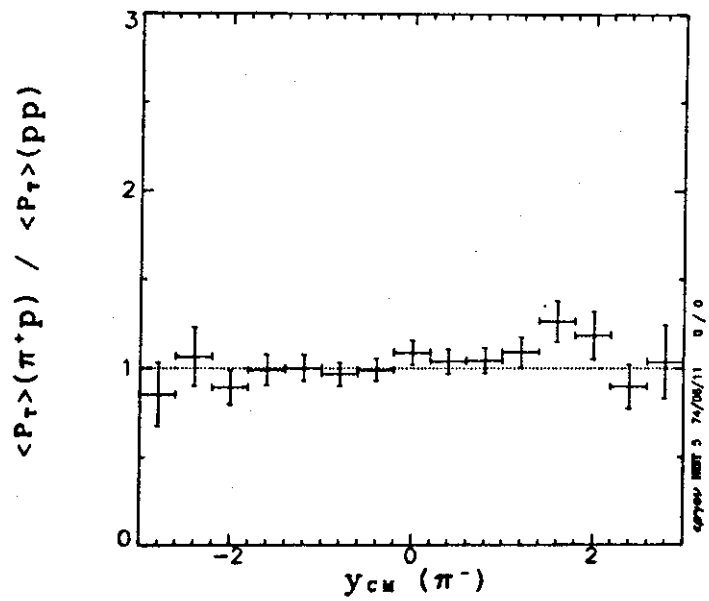

100 GEV/C $y_{CM}<0$

π^-

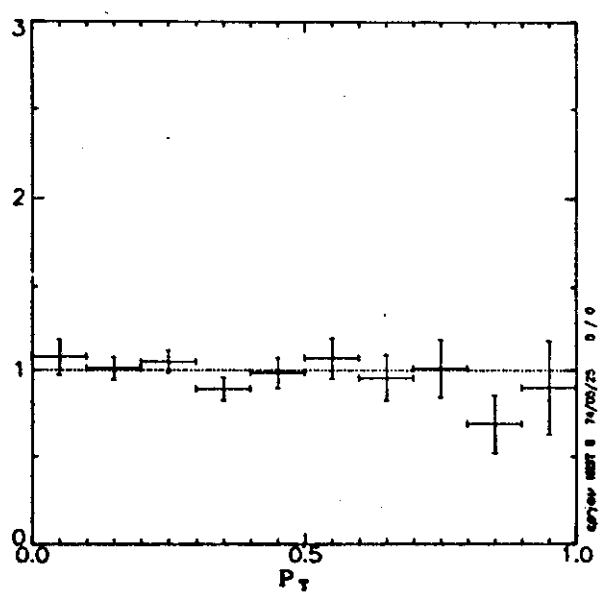

Fig. 3

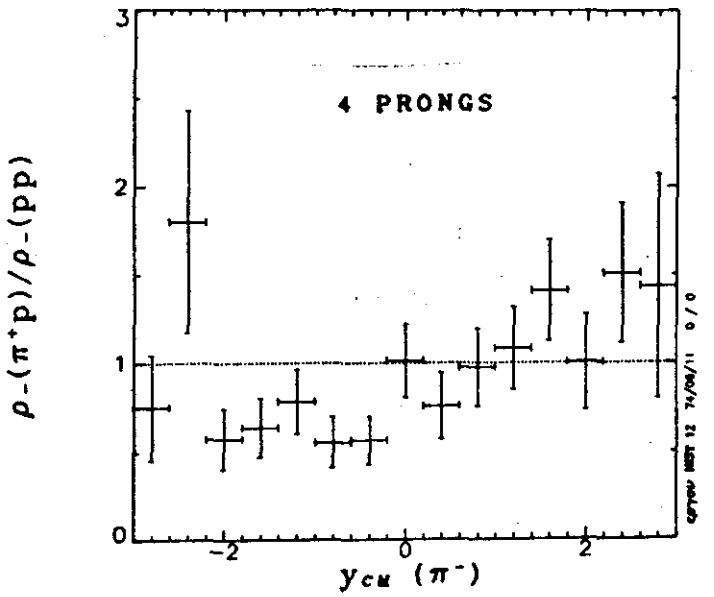
4 PRONGS
ρ-(π⁺p)/ρ-(pp)
y_CM (π⁻)
0
1
2
3
−2
0
2

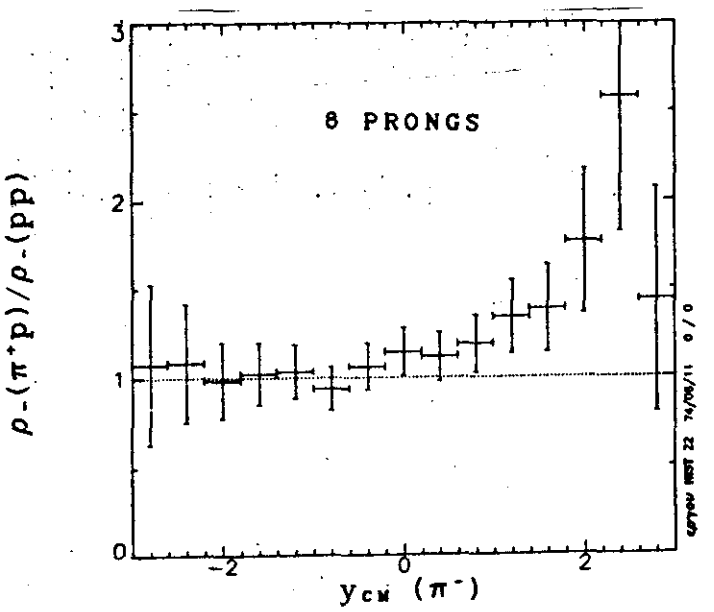
8 PRONGS
ρ-(π⁺p)/ρ-(pp)
y_CM (π⁻)
0
1
2
3
−2
0
2

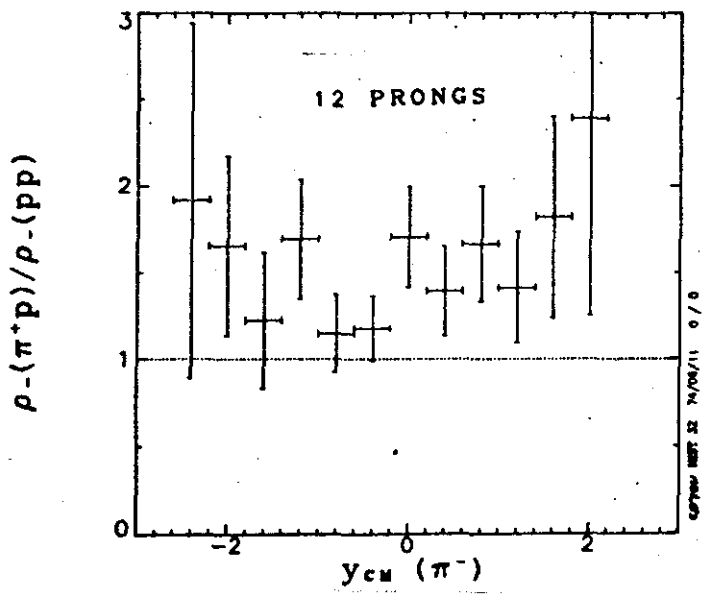
12 PRONGS
ρ-(π⁺p)/ρ-(pp)
y_CM (π⁻)
0
1
2
3
−2
0
2

Fig. 4

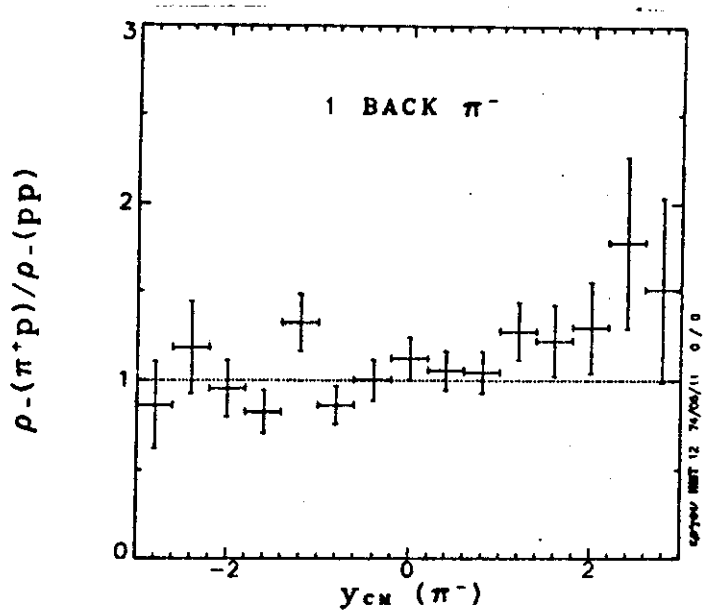
1 BACK π⁻
ρ-(π⁺p)/ρ-(pp)
y_CM (π⁻)
0
1
2
3
−2
0
2

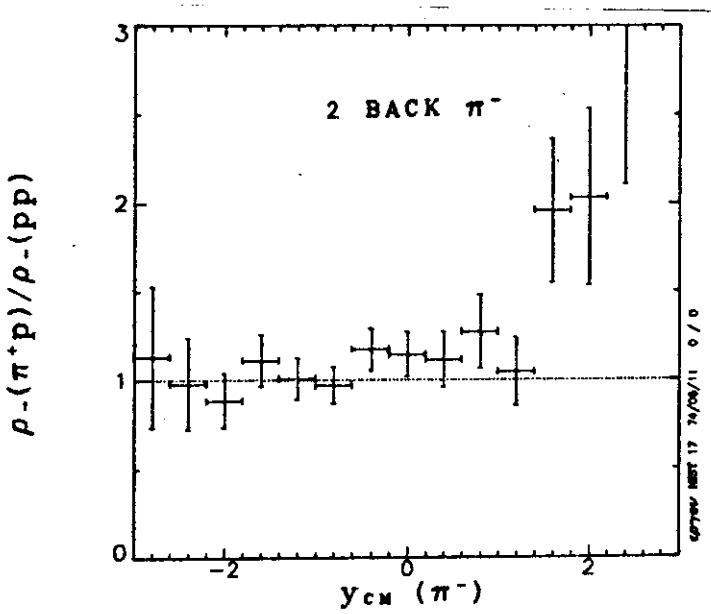
2 BACK π⁻
ρ-(π⁺p)/ρ-(pp)
y_CM (π⁻)
0
1
2
3
−2
0
2

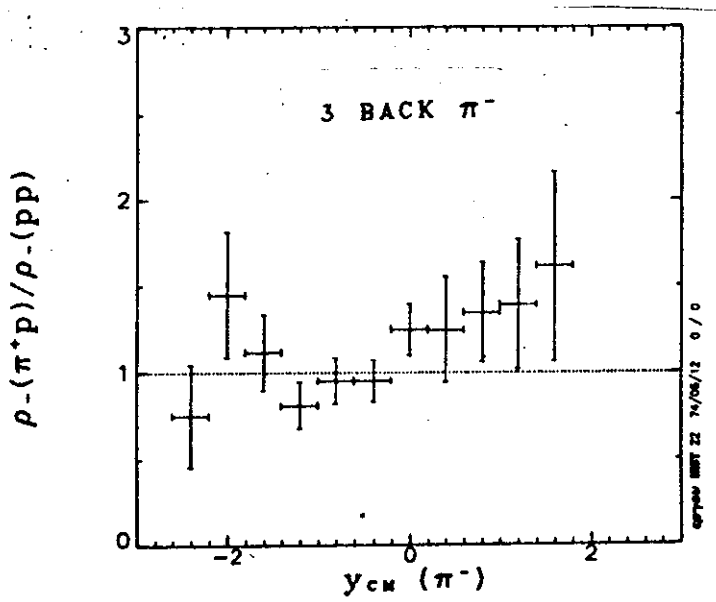
3 BACK π⁻
ρ-(π⁺p)/ρ-(pp)
y_CM (π⁻)
0
1
2
3
−2
0
2

Fig. 5.

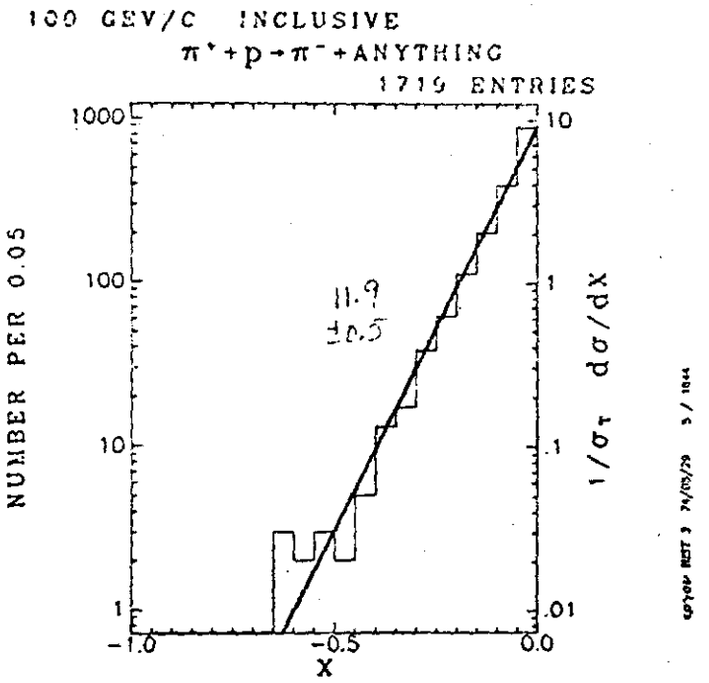
100 GEV/C INCLUSIVE
π⁺+p→π⁻+ANYTHING
1719 ENTRIES
NUMBER PER 0.05
1/σT dσ/dX
X
11.9
±0.5
1000
100
10
1
10
1
.1
.01
-1.0
-0.5
0.0

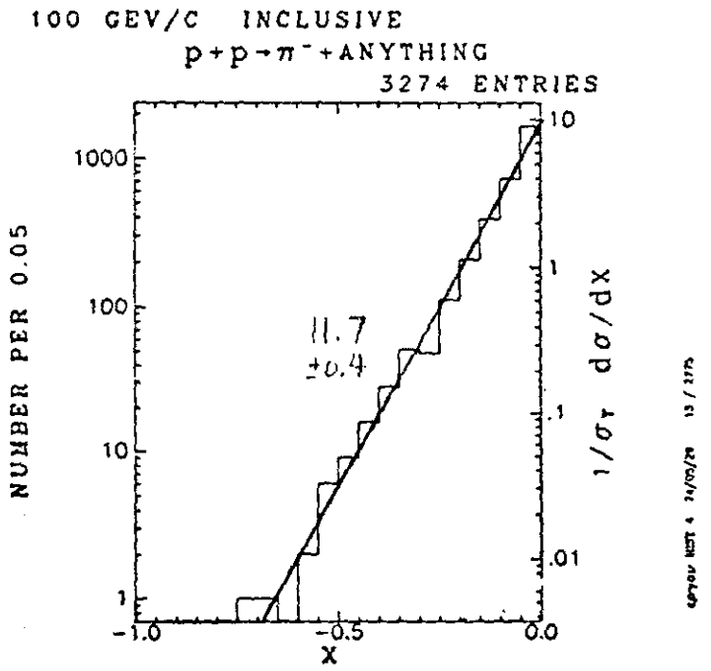
100 GEV/C INCLUSIVE
p+p→π⁻+ANYTHING
3274 ENTRIES
NUMBER PER 0.05
1/σT dσ/dX
X
11.7
±0.4
1000
100
10
1
10
1
.1
.01
-1.0
-0.5
0.0

Fig. 6

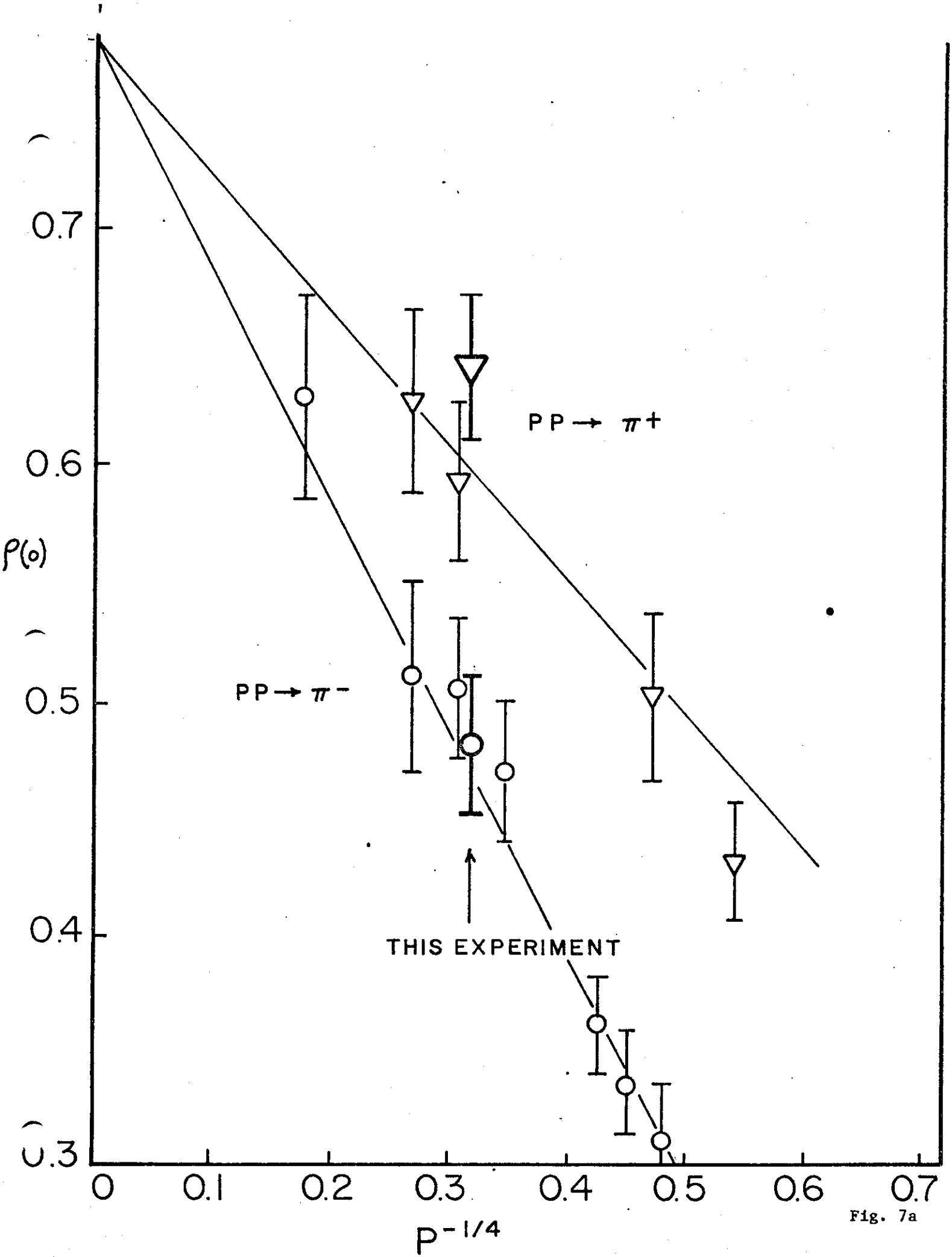
0.7
0.6
0.5
0.4
0.3
ρ(0)
PP → π+
PP → π−
THIS EXPERIMENT
0
0.1
0.2
0.3
0.4
0.5
0.6
0.7
P^-1/4

Fig. 7a

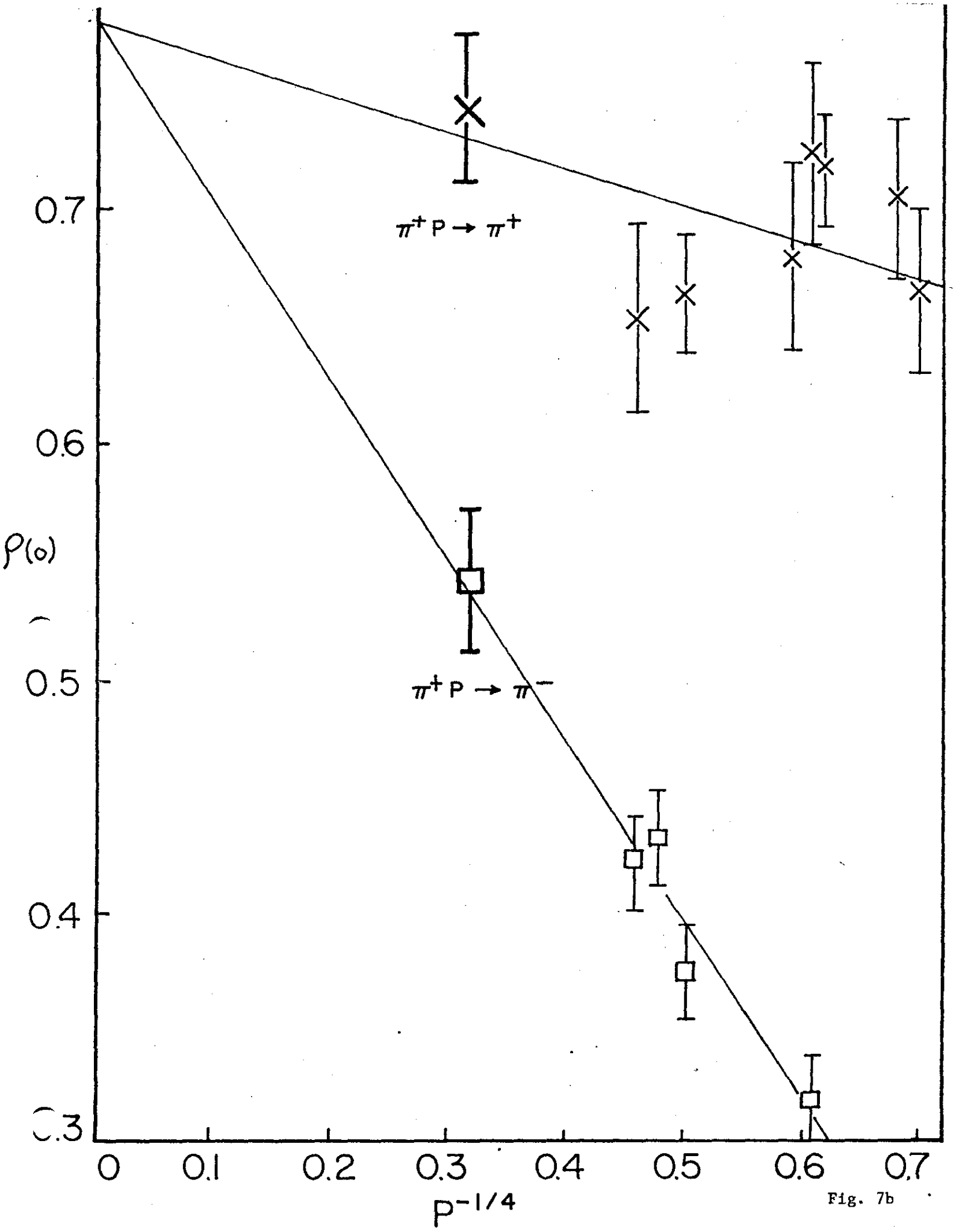

Fig. 7b

100 GEV/C INCLUSIVE

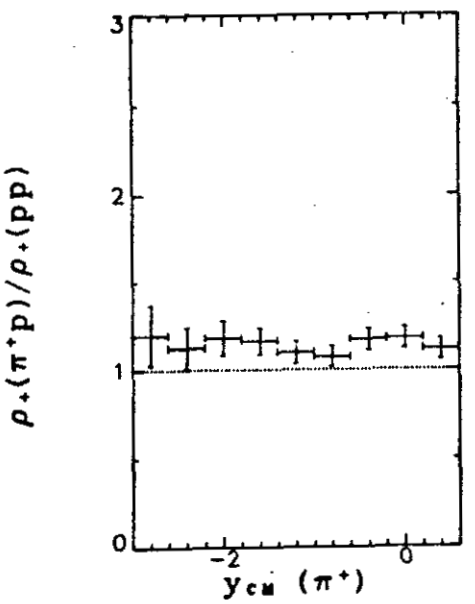

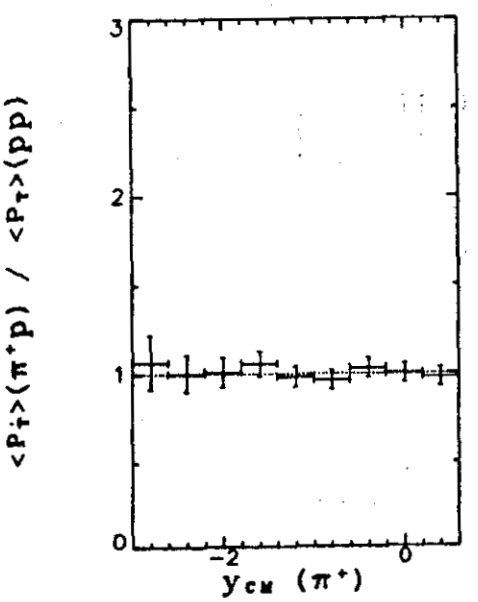

Fig. 8